

# RSC Advances



This is an *Accepted Manuscript*, which has been through the Royal Society of Chemistry peer review process and has been accepted for publication.

*Accepted Manuscripts* are published online shortly after acceptance, before technical editing, formatting and proof reading. Using this free service, authors can make their results available to the community, in citable form, before we publish the edited article. This *Accepted Manuscript* will be replaced by the edited, formatted and paginated article as soon as this is available.

You can find more information about *Accepted Manuscripts* in the [Information for Authors](#).

Please note that technical editing may introduce minor changes to the text and/or graphics, which may alter content. The journal's standard [Terms & Conditions](#) and the [Ethical guidelines](#) still apply. In no event shall the Royal Society of Chemistry be held responsible for any errors or omissions in this *Accepted Manuscript* or any consequences arising from the use of any information it contains.

## Efficient functionalization of gold nanoparticles by cysteine conjugated protoporphyrin IX for singlet oxygen production in vitro

Mohsen Ashjari<sup>1,2,\*</sup>, Soheila Dehfuly<sup>2</sup>, Daryoush Fatehi<sup>3</sup>, Ronak Shabani<sup>4</sup>, Morteza Koruji<sup>4</sup>

1. Chemical Engineering Department, Faculty of Engineering, University of Kashan, Kashan, Iran

Email: [ashjari.m@kashanu.ac.ir](mailto:ashjari.m@kashanu.ac.ir), [ashjari.m@gmail.com](mailto:ashjari.m@gmail.com)

Tel.: +98 31 55912494

Fax: +98 31 55912424

2. Institute of Nanoscience and Nanotechnology, University of Kashan, Kashan, Iran

[s.dehfuly65@gmail.com](mailto:s.dehfuly65@gmail.com)

3. Medical Physics Department, Faculty of Medicine, Shahrekord University of Medical Sciences, Shahrekord, Iran

[d.fatehi@yahoo.com](mailto:d.fatehi@yahoo.com)

4. Cellular and Molecular Research Center & Department of Anatomical Sciences, School of Medicine, Iran University of Medical Sciences, Tehran, Iran

[ronakshabani@yahoo.com](mailto:ronakshabani@yahoo.com), [koruji1@gmail.com](mailto:koruji1@gmail.com)

\* To whom all correspondence should be addressed

**Abstract**

Gold nanoparticles with suitable properties are supreme therapeutic agents and provide effective signal enhancement in photodynamic therapy (PDT). In this study, protoporphyrin IX (PpIX) conjugated gold nanoparticles (GNPs) were prepared using covalent conjugation by cysteine as adaptable linkage. The thiol group of cysteine was bound to the gold nanoparticles and also formation of the amide linkage between PpIX and cysteine was confirmed by FT-IR. The spectroscopic characterizations (FT-IR and UV-vis) proved the formation of the PpIX conjugated gold nanoparticles. The reaction process also was performed by the thin layer chromatography. Two different laser sources were used to activate the PpIX molecule in the ground state which was highly associated with the amount of produced singlet oxygen. Gold nanoparticles revealed a significant improvement in singlet oxygen production of PpIX molecule. The photocytotoxicity of the PpIX conjugated gold nanoparticle was also investigated using spermatogonial cells *in vitro*. The results ensure that designed PpIX conjugated gold nanoparticle has greatly provided an efficient agent for cellular photodynamic therapy.

**Keywords**

Gold nanoparticles, Cysteine, Protoporphyrin IX, Photodynamic therapy, Phototoxicity, *In vitro*.

## 1. Introduction

Photodynamic therapy (PDT) is a nondestructive approach of medical treatment which terminates cancerous and abnormal cells by combination of a photosensitizing molecule and light irradiation at an appropriate wavelength to production of reactive oxygen species [1,2,3]. The photosensitizing molecule becomes excited and then its energy is transferred to ground state molecular oxygen to produce reactive oxygen species (ROS) such as singlet oxygen ( $^1\text{O}_2$ ). Singlet oxygen can cause oxidation of amino acid, DNA, and lipid, leading cell destruction which forms the basis of PDT for cancer treatment [4]. The effectiveness of PDT has been determined by the efficiency of singlet oxygen production [5]. Many factors have influence on singlet oxygen production such as nature of the photosensitizer, light wavelength, light intensity and so on [6].

The nanotechnology was revolted PDT application, where nanoparticles e.g. gold nanoparticles (GNP) were used as multi-functional medicines [7]. Due to the large enhancement of the surface electric field on the metal nanoparticles surface, many applications such as PDT are possible. One of the main features of metal nanoparticles is their strong surface plasmon resonance (SPR) showing great promise for PDT.

The surface plasmon oscillation is a collective oscillation of the electrons in the conduction band. For gold nanoparticles the oscillation frequency is usually in the visible region rising to the strong surface plasmon resonance absorption. The plasmon resonance absorption has absorption coefficient orders of magnitude greater than strongly absorbing dyes [8].

Cysteine [cys,  $\text{HS-CH}_2\text{-CH}(\text{NH}_2)\text{-COOH}$ ] has an especially high affinity for gold due to its thiol (sulfhydryl) side chain, which enables bonding of drug to metal surfaces as a crosslinker. In combination with gold nanoparticles, it still retains biofunctionality through the amine and carboxylic groups. Functionalization of gold nanoparticles with cysteine leads to aggregation of nanostructures which generally attributed to the formation of zwitterions involving interaction of the deprotonated carboxylate and protonated amine groups of one cys-GNP with the opposite groups of cysteine absorbed on adjacent nanoparticles. Cysteine adsorbs as a fully protonated cation when deposited from acidic solution and as the fully deprotonated anion in basic solution [9]. A large number of synthetic routes are suitable for preparation of gold nanoparticle in the controlled manner [10-12]. Firstly Turkevich have demonstrated synthesized gold nanoparticle with a

diameter of 20 nm via reduction of  $\text{HAuCl}_4$  by trisodium citrate [13]. Sarangi et al. has studied fluorescent properties of gold nanoparticle capped with cysteine obtained by direct chemical reduction in presence of the amino acid [14].

Protoporphyrin IX (PpIX) is a model photosensitizing drug which has an absorption maximum of 410nm (soret band), along with four smaller peaks near 510, 540, 580 and 635 nm (Q bands), allowing for irradiation from multiple light sources with diverse spectral yields [15]. The carboxyl groups of the PpIX play an important role in the bioconjugation. Since the carboxyl groups are not directly attached to the porphyrin ring; due to conjugation, the esterifications of these groups has no direct effect on the electron distribution in the porphyrin ring and induces significant change in the light absorption and fluorescence spectra [16].

The tunable surface property of gold nanoparticles allows binding and carrying photosensitizers attached to their surface by covalent or non-covalent bonds and improve singlet oxygen production. Conjugation photosensitizers on gold nanoparticles surface was begun by Hone et al. in 2002 [17]. They have coated gold nanoparticles with a phthalocyanine photosensitizer which was shown to produce singlet oxygen with enhanced efficiency as compared to the free phthalocyanine. In an in vitro study, Gamaleia et al. reported that PDT activity of hematoporphyrin-gold nanoparticles is much higher than that of the original photosensitizer [18]. Ganesan et al. used glutathione (GSH) in gold nanoparticles synthesis for electrostatic and covalent conjugation of PpIX. They have conjugated folic acid to vector their complex and indicated the nanoparticle complexes are more phototoxic compared to free PpIX. Also they revealed that covalent complex being better than the two complexes and the folate-mediated nanocomplex is the superior of the studied complexes [6]. Eshghi et al. have described an efficient drug vector for photosensitizer delivery into the cells via synthesizing PpIX gold nanoparticles conjugates. They functionalized gold nanoparticles surface with 6-mercapto-1-hexanol to attach the PpIX molecule [19]. Wang et al. have demonstrated that due to increasing plasmon strength, conjugation of PpIX on gold nanoparticles surface enhanced ROS production [4]. Recently, they explored that gold nanoparticle aggregates for improving PDT efficiency in vitro which can be formed via electrostatic interaction. They were reported that ROS production by PpIX in the presence of aggregated was two times higher than the free PpIX

[5]. Hayden et al. studied electrostatic complexes with the plasmonic effect on PpIX activity applying rigid surface attachment using gold nanospheres and nanorods [20]. They found when PpIX is covalently bound close to the spherical nanoparticle surface, best enhancement occurs for photosensitizer activity.

Here, we investigated the relative increase in the PDT efficacy by PpIX conjugating with modified gold nanoparticles and using cysteine as a proper linker. We have synthesized cysteine modified gold nanoparticles (cys-GNPs) and we used covalent binding technique to conjugate PpIX on the surface of the gold nanoparticles. Furthermore, we have studied singlet oxygen and PDT efficacy of the synthesized PpIX-conjugated cysteine-modified gold nanoparticles (PpIX-cys-GNPs) against a fluorescent probe (anthracene) and spermatogonial cells in vitro, respectively.

## 2. Experimental section

### 2.1. Materials

Hydrogen tetrachloroaurate (III) trihydrate ( $\text{HAuCl}_4 \cdot 3\text{H}_2\text{O}$ ) 99.5%, L-cysteine, trisodium citrate and anthracene were obtained from Merck Millipore. Protoporphyrin IX, N-hydroxy succinimide (NHS), 1-ethyl-3-(3-dimethylaminopropyl)- carbodiimide hydrochloride (EDC), dimethyl sulfoxide (DMSO) and methyl thiazolyldiphenyl-tetrazolium bromide (MTT) were purchased from Sigma–Aldrich (St Louis, MO, USA). Deionized water was used in all aqueous solutions and rinsing procedures. All other chemicals and solvents were analytical grade and used without further purification.

### 2.2. Preparation of cysteine modified gold nanoparticles (cys-GNPs)

Gold nanoparticles were prepared by a reduction of  $\text{HAuCl}_4$  using trisodium citrate as the reducing then stabilizing agent [13]. Briefly, 12.5 mL of sodium citrate solution (38.8 mM) was quickly introduced to 125 mL of freshly boiled aqueous solution of 1 mM  $\text{HAuCl}_4 \cdot 3\text{H}_2\text{O}$  under vigorous stirring. The solution was heated and stirred for another 15 min, during which time its color changed from pale yellow to wine red. The obtained solution was cooled to room temperature while being stirred continuously until reduction reaction was completed. In order to surface modification, 0.1 mL of cysteine solution (2.4

mM) was added to 5 ml of the solution and the mixture was stirred for 4 h without any change in color. Finally gold nanoparticles functionalized with cysteine (cys-GNPs) were kept and stored in R.T. for further conjugation.

### **2.3. Preparation of PpIX conjugated gold nanoparticles (PpIX-cys-GNPs)**

In order to chemical conjugation of PpIX to amine group of cysteine on the surface of the gold nanoparticles, activation carboxyl group of PpIX is needed [5]. First, 1 mg of PpIX was dissolved in 3 mL DMSO, followed by the addition 2.3 mg of EDC and 1.7 mg of NHS into solution. After the complete dissolution, 5mL of solution cys-GNPs was added to the stirring mixture and was allowed to continue for overnight at room temperature forming water-dispersable PpIX-cys-GNP conjugate and store in 25 °C for further characterization.

### **2.4. The singlet oxygen measurement**

To detect and qualitatively measure of the singlet oxygen level, a fluorescent probe, anthracene was used. This probe is fluorescent; however it turns into non-fluorescent anthraquinone after being oxidized by singlet oxygen. Initially, anthracene 0.4 mg was dissolved in methanol 10 mL at 50 °C. Then 100 $\mu$ L of anthracene solution (0.1 mM) introduced to 3 mL free PpIX solution and the water-dispersed PpIX-Cys-GNP conjugates for 60 min before irradiation. In the next step the solutions placed under L530 (solid-state laser, green) and L633 (gaseous HeNe laser, red) light irradiation with a fixed power density (5 and 17 mW respectively) for 20 min. Furthermore, the samples were further incubated for 20 min at ambient temperature and then the emission spectrum of the anthracene was recorded by photoluminescence spectrometer. The produced singlet oxygen amount was measured by decreasing fluorescence intensity.

### **2.5. Experimental animals**

In this experiment, 20 neonatal mice (3-6 days old) old were used. Male neonate National Medical Research Institute (NMRI) mice were obtained from stocks of Razi Laboratory (Tehran, Iran) and moved to the animal house of Iran University of Medical Sciences (Tehran, Iran). They were housed in polycarbonate cages in a room at a temperature range

of 22°C–25°C, with a 12-hour light/dark cycle. The mice could freely reach drinking water and standard laboratory pellets. National Research Council guidelines were carefully considered during the research.

## **2.6. Isolation and cultivation of spermatogonial stem cells**

Testes from the 3-6 day-old NMRI mice were collected for the preparation of cell suspension following enzymatic digestions and purification steps. After decapsulation, the testes were minced and suspended in Dulbecco's Modified Eagle Medium/F12 (DMEM/F12) (Gibco, USA) supplemented with 2.438 g/L NaHCO<sub>3</sub>, single-strength nonessential amino acids, penicillin (100 IU/ml), streptomycin (100 µg/ml), and gentamycin (40 µg/ml) (all from Life Technologies).

Testicular cells were separated by the method of van Pelt et al. (1996) with minor modifications (24). Briefly, minced testis pieces were suspended in DMEM/F12 containing 0.5 mg/mL collagenase/dispase, 0.5 mg/mL Trypsin, and 0.05 mg/mL DNase, for 30 minutes (with shaking and a little pipetting) at 37°C. All enzymes were purchased from Sigma-Aldrich. For the next step, the interstitial cells were removed by washing and centrifuging for 1 min at 1500 rpm (two–three times) DMEM/F12 medium. A second digestion step was performed in DMEM/F12 media by adding a fresh enzyme solution into the seminiferous cord fragments as previously described. After cell separation and filtration through 70 µm nylon filters, the collected cells were used for the culture cells. Sertoli cells and myoid cells were also isolated through overnight differential plating in DMEM/F12 containing 10% fetal calf serum (FCS). After the removal of the Sertoli and myoid cells, spermatogonia, which remained in suspension, were collected and cultured in DMEM/F12 containing 1% FCS and 20 ng/mL GDNF and bFGF 10 ng/ml for 2 weeks. The cells were incubated at 32°C, 5% CO<sub>2</sub> in a humidified atmosphere, and the medium was refreshed three times per week.

## **2.7. Cell viability assay**

In order to photocytotoxicity assay spermatogonial cells were divided into four groups: control (no PpIX and no laser irradiation), sham (only laser irradiation), PpIX-cys-GNPs and free PpIX (0.1 mL of 0.125 mg/mL). After that, cells viability was evaluated with



MTT assay. Spermatogonial cells were seeded into 96-well plate at a density of  $20 \times 10^3$  cells/well/0.2 mL. To assess the effect of PpIX activity in exposure time, the cells were treated with the samples and incubated cells for 12 hours. After the incubation, all trials (except control) were irradiated with a HeNe laser ( $633 \text{ nm}$ ,  $15 \text{ mW/cm}^2$ ) for 20 min. Incubation was continued for an additional overnight in dark condition. Then the cells were centrifuged, the wells were washed twice with PBS. MTT tetrazolium salt was prepared freshly ( $5 \text{ mg/mL}$  MTT tetrazolium salt and diluted with DMEM/F12 containing 2% FBS). Then a 0.2 mL of the prepared solution was added to each well and they were incubated for 4 h at  $37 \text{ }^\circ\text{C}$ , leading to the formation of formazan dye, followed by the centrifuge of the solution and the supernatant removal. The MTT formazan crystals were then dissolved in DMSO (0.1 mL) for 15 min in a micro titer plate shaker. Thereafter, the optical density (OD) was measured with an ELISA reader (Thermo Electron) at  $570 \text{ nm}$  as the reference and test wavelengths. The viable rate was calculated by the following equation:

$$\text{Viable rate} = (\text{OD}_{\text{treated}}/\text{OD}_{\text{control}}) \times 100$$

Where  $\text{OD}_{\text{control}}$  was obtained in the absence of laser irradiation and photosensitizer.

## 2.8. Equipment

The absorbance measurements were performed with a Shimadzu UV-2100 spectrophotometer. FT-IR spectra were recorded on a 102MB BOMEM apparatus. The X-ray diffraction pattern was obtained on X'Pert pro multipurpose diffractometer (MPD) using Cu-K $\alpha$  radiation. The morphology and size of the gold NPs was performed on a MIRA3 FEG scanning electron microscope (SEM). Thin-layer chromatography (TLC) was performed using precoated silica gel plates (Merck Kieselgel 60F254). Fluorescence spectra of the anthracene were recorded on a photoluminescence spectroscopy (Perkin Elmer LS55) at ambient temperature. In other to excite PpIX molecules two illuminate source was used: helium-neon laser (HNL-150R) and solid-state laser (MC2000) and then the emitted fluorescence was detected.

## 3. Results and discussion

The conjugation of PpIX to cysteine modified gold nanoparticles can be conducted using the EDC/NHS reaction as shown in Fig. 1. Appropriate linkage is necessary for selective targeting of abnormal cells and photosensitizer conjugating to nanoparticles efficiently. Cysteine was used to create linkage between the gold nanoparticles and PpIX. Since cysteine is bifunctional, when it conjugate to nanoparticles it has another functional group for attaching a tumor-specific ligand, such as folic acid. Conjugation of PpIX to GNPs was followed by TLC. Monitoring the conjugation by TLC analysis indicated progressive disappearance of the PpIX and the formation of the PpIX-cys-GNPs. When PpIX conjugate to GNPs, because of heavy gold nanoparticles attached, PpIX-cys-GNPs molecules cannot present on TLC.

### Figure 1

#### 3.1. XRD and SEM analysis of gold nanoparticles

X-ray diffraction (XRD) analysis has been used to study structure of prepared gold nanoparticles. Fig. 2a shows a representative XRD pattern of the gold nanoparticles prepared by the trisodium citrate as a reducing agent. The XRD peaks are found to be broad indicating the formation of nanoparticles. Five diffraction peaks are observed which can be indexed to the (111), (200), (220) and (311) reflections of face centered cubic (fcc) structure of metallic gold. Moreover, the intensity of the (111) diffraction was much stronger than those of the (220), (200) and (311) diffractions. The XRD pattern, thus clearly reveals that the synthesized gold nanoparticles were essentially crystalline. However, there was no impurity in the pattern (Fig. 2a). The average particle size of gold nanoparticles can be calculated using Debye–Scherrer equation which is found to be around 14.1 nm [21].

Scanning electron microscope (SEM) has been applied to identify the size, shape, and morphology of gold nanoparticles. The SEM image (Fig. 2b) of gold nanoparticles demonstrates that almost spherical shaped particles are more abundant than other shapes. Additionally, these nanoparticles were monodispersed and had an average diameter of roughly 20 nm. This result was consistent with obtained XRD results.

### Figure 2

### 3.2. FTIR analysis

The interaction of prepared gold nanoparticles with cysteine as well as PpIX conjugation were confirmed by FT-IR spectroscopy as shown in Fig. 3. Cysteine molecule has a characteristic stretching vibration at  $2550\text{ cm}^{-1}$ , which is associated with S-H bond (thiol group). As shown in FT-IR spectrum of prepared cys-GNPs (Fig. 3 lower), this peak disappears which is due to S-H bond breakage. This confirms bond formation of cysteine and gold nanoparticles from S head groups. Conjugation of PpIX molecules on surface of the modified gold nanoparticles was followed by formation of amide group in the presence of EDC and NHS as coupling agents and appearance of its characteristic peaks. On covalent bonding of the carboxyl group of PpIX molecules with the amine groups of the cysteine, the FT-IR spectrum of the PpIX-cys-GNPs (Fig. 3 upper) represents the carbonyl group peak at  $1640\text{ cm}^{-1}$  (C=O stretch) and C-N in  $1400\text{ cm}^{-1}$  which confirms the formation of amide bond.

**Figure 3**

### 3.3. UV-vis absorption study

Absorption spectroscopy is an effective method to determine the formation and stability of gold nanoparticles in colloidal aqueous solution. Colloidal solutions of gold nanoparticles have intense color due to surface plasmon resonance (SPR). The position of SPR band in UV-vis spectra is sensitive to particle size, shape and local refractive index [22].

The UV-vis spectrum of gold nanoparticle synthesized by trisodium citrate in aqueous medium is shown in Fig. 4 (curve a). The average particle size of gold nanoparticle was 14.66 nm which calculated using equation proposed by Hiss ( $5.6 \times 10^{12}$  gold particles per one liter) [23].

The absorption spectrum gold nanoparticles after modification with cysteine (cys-GNPs) is seen in Fig. 4 (curve b). The absorption peak of the cys-GNPs was 630 nm, which had red-shifted 10 nm in comparison to the absorption peak of the gold nanoparticles. This change might be due to the aggregate size and interparticles distance. When the interparticles distance in the aggregates decreased, fewer than about the average particle diameter, the electric dipole-dipole interaction and coupling between the plasmons of neighboring particles in the aggregates resulted in the bathochromic shift of the absorption band [10].

In order to study stability of cys-GNPs, we again analyzed them after three days (see supporting information) and it is observed cys-GNPs was unstable and aggregate. The positively charged amino group in cysteine ( $-\text{NH}_3^+$ ) might be interacted with the negative charge ( $\text{COO}^-$ ) on the surface of the other gold nanoparticles through electrostatic binding, therefore forming assemblies and aggregates [10].

The absorption spectra of PpIX and PpIX-cys-GNPs are shown in Fig. 4b. The absorption spectrum of PpIX illustrated its characteristic peak at 400 nm, 508 nm, 560 nm and 610 nm. The PpIX-cys-GNPs conjugate showed the absorption peaks are red shifted to 25 nm with respect to the PpIX spectrum before the conjugation. This red shift could be due to the covalent attachment of the PpIX molecule on the surface of the GNPs. Moreover, it attributed to the coupling of the individual surface plasmon of nanoparticles in the aggregated structures, which will observed if the inter-linked nanostructures are formed [19]. It is also observed that there was an increase in the absorption intensity of the some peaks of the PpIX-cys-GNPs conjugate with respect to that of the PpIX molecule. This increase might be attributed to the change in the surrounding media and presence the amine groups (electron donate) [6]. The results conformed FTIR analysis and observed changes in absorption spectra. Furthermore these results provided indirect evidence on the formation of the PpIX-cys-GNPs.

#### Figure 4

#### 3.4. Measurement of singlet oxygen

The singlet oxygen production is of greatest importance in PDT and its measurement presents an indication of how well a photosensitizing molecule is able to produce ROS. To produce suitable singlet oxygen energy transfer with efficient rate is required between the excited state of the photosensitizer and the ground state of oxygen molecules. Anthracene as singlet oxygen quencher used to measure the singlet oxygen by changing in the emission spectra when it has exposure to ROS. As a result, anthraquinone generates has no fluorescence property in contrast to the anthracene. Actually, the decreasing emission intensity of anthracene represents the singlet oxygen production. In order to activate PpIX molecule, the prepared PpIX-cys-GNPs stimulated using light sources. For comparison,

two light sources of helium–neon laser (L530nm) and solid-state laser (L633nm) were applied to indicate efficient energy transfer.

Figure 5 illustrates decreasing of anthracene intensity inducing produced singlet oxygen by the free PpIX and PpIX-cys-GNPs when they were irradiated for 20 min. Evolution of the emission intensity of the anthracene demonstrated both of free PpIX and PpIX-cys-GNPs have been produced singlet oxygen. However, the PpIX-cys-GNPs produced more oxygen singlet in comparison with the free PpIX. This could be due to the nature of the chemical binding of the PpIX to the surface of the nanoparticles. Because of surface plasmon of the gold nanoparticles, highly efficient energy transferring to the PpIX molecule can be occurred in the ground state, resulting in the excited state, consequent in the production of singlet oxygen [20]. Thus, using gold nanoparticles is an effective tool for enhancing singlet oxygen production and the PDT efficacy.

The effect of the irradiation sources on the singlet oxygen production is shown in Fig. 6. According to this observation, both free PpIX and PpIX-cys-GNPs could more adsorb irradiation from L633. It is resulted for our prepared conjugate; L633 in comparison with the L530 can produce larger amounts of singlet oxygen.

**Figure 5**

**Figure 6**

### **3.5. In vitro PDT efficiency**

The in vitro PDT efficiency of free PpIX and PpIX-cys-GNPs was evaluated against spermatogonial cells using the MTT assay technique (MTT, 3-(4,5-dimethylthiazol-2-yl)-2,5-diphenyltetrazolium bromide). The concentrations of samples were constant (1 g/ml) and the percentages of photocytotoxicity were determined. It is well-known that cell destruction in PDT treatment is correlated with the singlet oxygen level [17]. With the increase of intracellular singlet oxygen level caused by gold nanoparticles, higher cell destruction is expected.

Figure 7 reveals the photocytotoxic effect of the free PpIX molecule and PpIX-cys-GNPs. Following PDT, 76% cell viability was observed for the PpIX molecule whereas 41% cell viability was found for the PpIX-cys-GNPs. This could be related to lowering of singlet oxygen production. The control and sham group cells showed a minimal photocytotoxicity

effect with a cell viability of 99% and 97% respectively. In this study we found that only with light exposure and without any photosensitizer (control and sham samples respectively) demonstrated no detectable photocytotoxicity.

These results confirm that the presence of gold nanoparticles with highly plasmonic resonance in PpIX-mediated PDT treatment could significantly enhance the cell destruction efficacy and the improved PDT efficacy. Moreover, the covalent linkage owing to the cysteine between PpIX and gold nanoparticles shows increase in the photocytotoxic effect, as a result of the stable binding nature; enhance PDT efficiency and hence promoting cellular uptake [5]. Further, studies have reported that the stability of nanoparticle is crucial in enhancing the uptake of the photosensitizer. However, conjugation increases the solubility of the PpIX and thereby increasing the PDT efficacy [19].

### Figure 7

#### 4. Conclusion

This study shows that gold nanoparticles in combination with cysteine compound provide a simple way for the conjugation of PpIX and enhanced PDT efficacy. The preparation of cysteine modified gold nanoparticles was considered using morphological (SEM) and structural (XRD) evaluation techniques and these results proved the formation of the cys-GNPs. TLC analysis was indicated that all of the PpIX had been consumed and conjugated to gold nanoparticles. The cysteine linkage is playing important role for controlling the stabilization of the gold nanoparticles due to thiol group. The cys-GNP can be attributed to chemical binding with the PpIX molecule. The spectroscopic studies (FT-IR and UV-vis) were confirmed that bioconjugation between carboxyl groups of the PpIX molecule with amine group remain on surface of metal ion. The singlet oxygen produced was detected by the change in the anthracene spectra. We demonstrated that singlet oxygen production by light irradiation of PpIX photosensitizer is significantly enhanced by gold nanoparticle conjugates. The PpIX-cys-GNP conjugates were uptaken by spermatogonial cells in vitro and their photocytotoxicity was also investigated. The designed nanostructured PpIX conjugate has provided an efficient agent for PDT which makes it potential candidates for cancer treatment.

### **Acknowledgements**

This work was funded by the University of Kashan. The authors would like to thank Dr. Mehrdad Moradi (University of Kashan) for his assistance in the laser instrument and his kind cooperation. Authors declare that there is no conflict of interest in this study.

## References

1. O. J. Stacey and J. A. S. Pope, *RSC Advances*, 2013, **3**, 25550.
2. S. S. Lucky, K. C. Soo, and Y. Zhang, *Chem. Rev.*, 2015, **115**, 1990.
3. K. Han, J-Y Zhu, S-B Wang, Z-H Li, S-X Cheng and X-Z Zhang, *J. Mater. Chem. B*, 2015, DOI: 10.1039/C5TB01659B.
4. M. Khaing and Y. Yang, *ACS Nano*, 2012, **6**, 1939.
5. Y. Yang, Y. Hu, H. Du and H. Wang, *Chem. Commun.*, 2014, **50**, 7287.
6. S. W. Prasanna, G. Poorani, R. A. Prakasa, M. Elanchezhian and S. Ganesan, *J. Nanosci. Nanotechnol.*, 2015, **15**, 5577.
7. De Bechet, P Couleaud, C. Frochot, M-L. Viriot, F. Guillemin and M. Barberi-Heyob, *Trends Biotechnol.*, 2008, **26**, 612.
8. S. Eustis and M. A. El-Sayed, *Chem. Soc. Rev.*, 2006, **35**, 209.
9. A. Ihs and B. Liedberg, *J. Colloid Interface Sci.*, 1991, **144**, 282.
10. R. G. Acres, V. Feyer, N. Tsud, E. Carlino, and K. C. Prince, *J. Phys. Chem. C*, 2014, **118**, 10481.
11. S. D. Luthuli, M. M. Chili, N. Revaprasadu and A. Shonhai, *IUBMB Life*, 2013, **65**, 454.
12. A. Majzik, R. Patakfalvi, V. Hornok and I. Dékány, *Gold Bulletin*, 2009, **42**, 113.
13. J. Turkevich, *Gold Bulletin*, 1985, **18**, 86.
14. S.N. Sarangi, A.M.P. Hussain and S.N. Sahu, *Appl. Phys. Lett.*, 2009, **95**, 073109/1.
15. A. E. OConnor, W. M. Gallagher and A. T. Byrne, *Photochem. Photobiol.*, 2009, **85**, 1053.
16. K. Kadish, R. Guilard and K. Smith (ed.), *The Porphyrin Handbook*, 1999, Vol. 2, 1st Ed, Elsevier.
17. D.C. Hone, P.I. Walker, R.E. Gowing, S. F. Geral, A. Beeby, I. Chambrier, M. J. Cook and D. A. Russell, *Langmuir*, 2002, **18**, 2985.
18. N. Gamaleia, E. Shishko, G. Dolinsky, A. Shcherbakov, A. Usatenko and V. Kholin, *Exp. Oncol.*, 2010, **32**, 44.
19. H. Eshghi, A. Sazgarnia, M. Rahimizadeh, N. Attaran, M. Bakavoli and S. Soudmand, *Photodiagn Photodyn.*, 2013, **10**, 304.
20. S. C. Hayden, L. A. Austin, R. D. Near, R. Ozturk and M. A. El-Sayed, *J. Photoch. Photobiol. A*, 2013, **269**, 34.
21. S. Aswathy and D. Philip, *Spectrochim. Acta A*, 2012, **97**, 1.
22. F. Chai, C. Wang, T. Wang and Z. Ma, *Nanotechnology*, 2010, **21**, 025501.
23. Y. Qiu, Shao. Liu, L. Kong and Z. Liu. *Spectrochim. Acta A*, 2005, **61**, 2861.



## Legends for Figures

Fig. 1. Schematic illustration of conjugation of PpIX to cysteine modified gold nanoparticle

Fig. 2. Structural and morphological analysis of gold nanoparticles, respectively: XRD pattern (a) and SEM image (b)

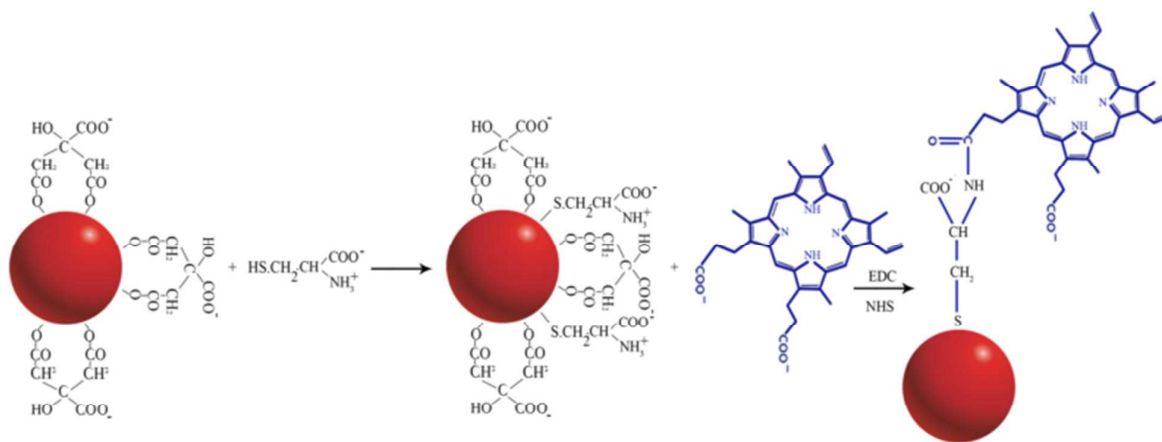
Fig. 3. FT-IR spectra of cys-GNPs (lower) and PpIX-cys-GNPs (upper)

Fig. 4. Absorption Spectra of the synthesized gold nanoparticle (a-dark), cys-GNP (a-gray), PpIX (b-dark) and PpIX-cys-GNP (b-gray)

Fig. 5. Reduction of anthracene intensity causing produced singlet oxygen by the PpIX and PpIX-cys-GNPs when they were irradiated by the lasers (L530 and L633) for 20 min

Fig. 6. Different sources (L530 and L633) for irradiation of samples and emission intensity changing of anthracene

Fig. 7. Viability of spermatogonial cells determined by MTT assay after PDT treatments where cells were incubated with samples for 4 h, and then irradiated for 20 min under a HeNe laser (633 nm, 15 mW/cm<sup>2</sup>). Subsequently, the cells were cultured for 24 h prior to MTT test.



**Fig. 1**

Fig. 1. Schematic illustration of conjugation of PpIX to cysteine modified gold nanoparticle

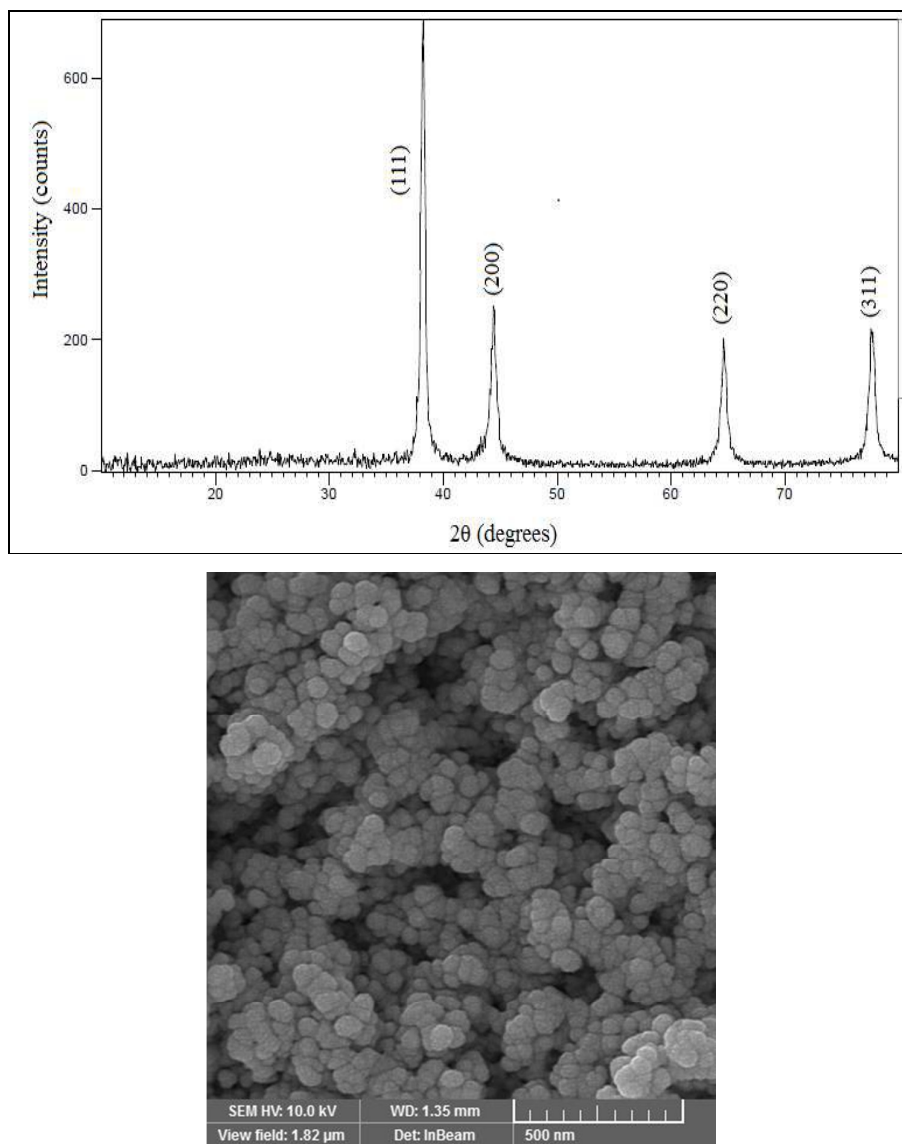
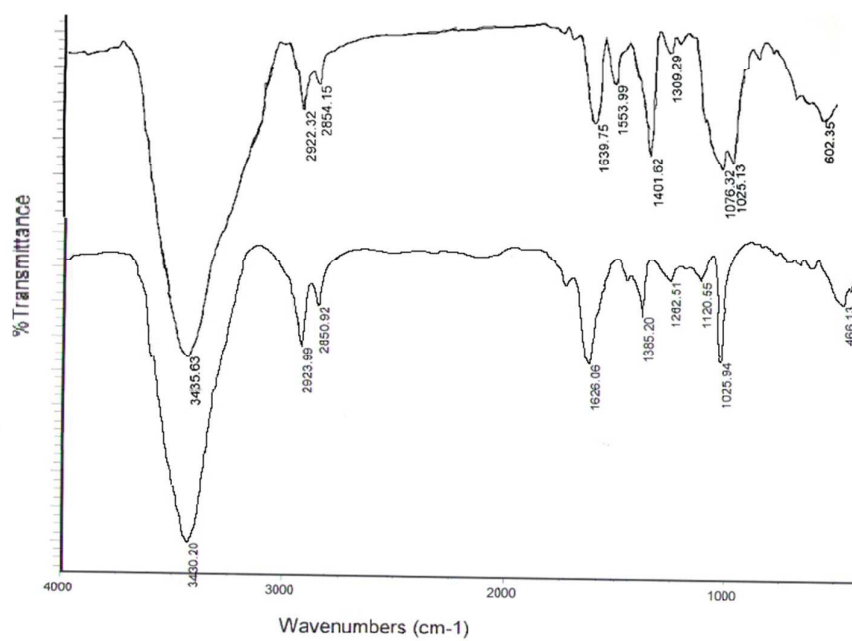
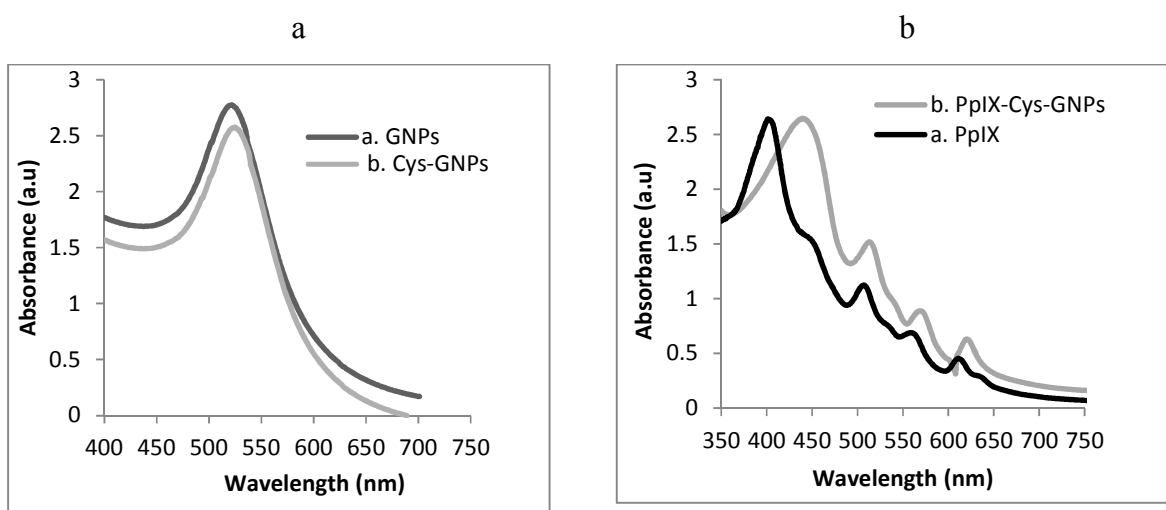
**Fig. 2**

Fig. 2. Structural and morphological analysis of gold nanoparticles, respectively: XRD pattern (a) and SEM image (b)



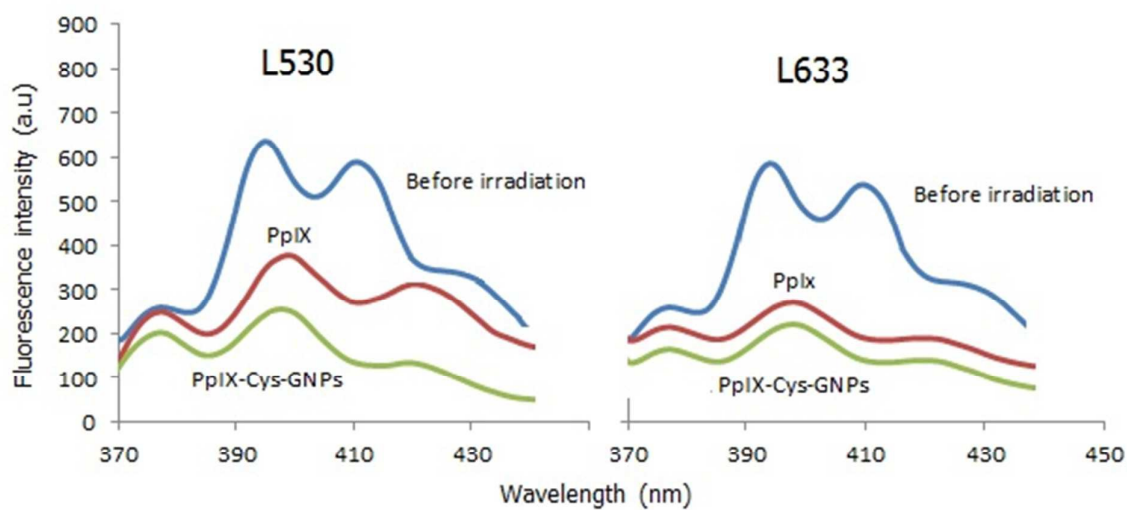
**Fig. 3**

Fig. 3. FT-IR spectra of cys-GNPs (lower) and PpIX-cys-GNPs (upper).



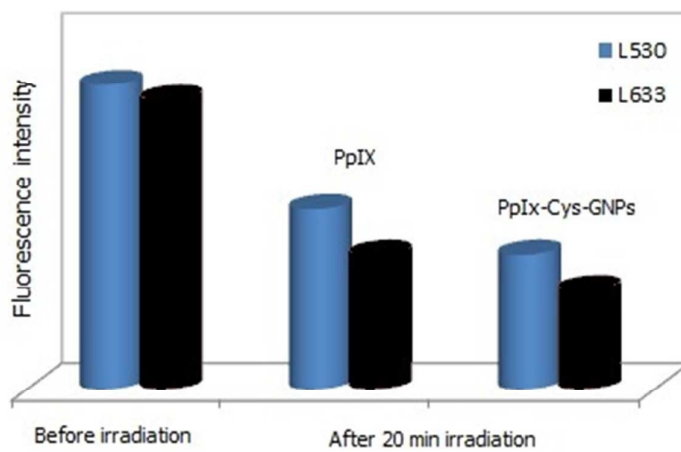
**Fig. 4**

Fig. 4. Absorption Spectra of the synthesized gold nanoparticle (a-dark), cys-GNP (a-gray), PpIX (b-dark) and PpIX-cys-GNP (b-gray)



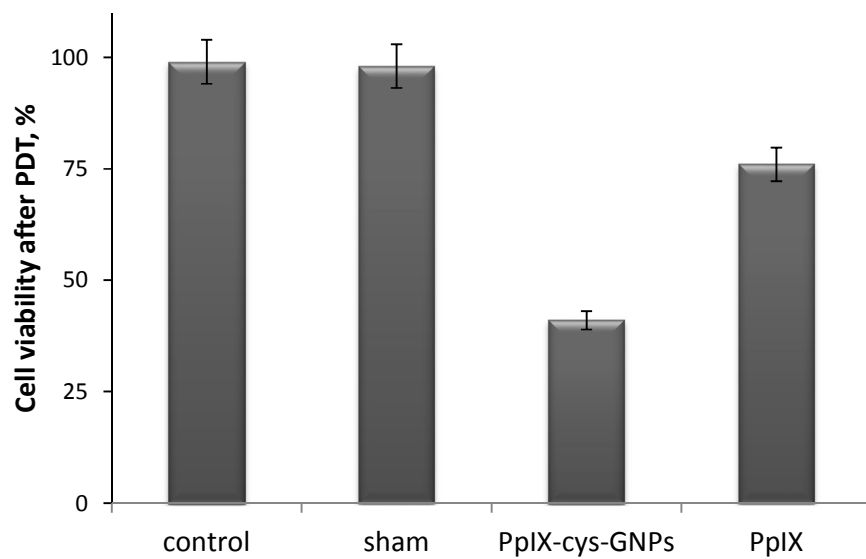
**Fig. 5**

Fig. 5. Reduction of anthracene intensity causing produced singlet oxygen by the PpIX and PpIX-cys-GNPs when they were irradiated by the lasers (L530 and L633) for 20 min.



**Fig. 6**

Fig. 6. Different sources (L530 and L633) for irradiation of samples and emission intensity changing of anthracene.



**Fig. 7**

Fig. 7. Viability of spermatogonial cells determined by MTT assay after PDT treatments where cells were incubated with samples for 4 h, and then irradiated for 20 min under a HeNe laser (633 nm, 15 mW/cm<sup>2</sup>). Subsequently, the cells were cultured for 24 h prior to MTT test.



## Graphical Abstract

M. Ashjari et al.

Efficient functionalization of gold nanoparticles by cysteine conjugated protoporphyrin IX for singlet oxygen production in vitro

